

Modeling of new grating designs for self-pulsating DFB lasers

M. Radziunas^{a,b}, H.-J. Wünsche^a, B. Sartorius^c, H.-P. Nolting^c
K. Schneider^b, O. Brox^c, D. Hoffmann^c

^a Institut für Physik der Humboldt-Universität zu Berlin, Invalidenstr. 110, D-10115 Berlin, Germany,
Phone: +49 30 20937649, Fax: +49 30 20937886, email: ede@physik.hu-berlin.de

^b Weierstraß-Institut für Angewandte Analysis und Stochastik Berlin, Mohrenstr. 39, D-10117 Berlin, Germany

^c Heinrich-Hertz-Institut für Nachrichtentechnik Berlin, Einsteinufer 37, D-10587 Berlin, Germany

Introduction: Multisection DFB lasers showing high-speed self-pulsations (SP) have opened a new field for the optical clock recovery at high bit rates. The basic effect was discovered in 1992 with 2-section devices [1]. Since then, optimization of the devices led to much improvement and the system capability has been demonstrated [2]. The present generation of devices is AR-coated and consists of two DFB sections and one phase section integrated in between (Fig. 1). The two DFB sections are basically identical, only lengths and pump levels are different. The longer one is pumped highly and provides the gain for lasing. The shorter DFB section is driven close to its gain transparency and acts as a dispersive reflector. The center section has neither an $1.55\mu\text{m}$ active layer nor a grating and serves as a passive phase tuning section.

Devices of this type have not been modeled yet. Our former modeling was based on a single mode approximation and considered devices with the gain section in the center and a reflecting facet adjacent to the phase section [3, 4]. In this paper we describe an improved model that properly takes into account all relevant modes and allows to treat a wider range of operation. Second, it is demonstrated that this model describes well and in good correspondence with the experiments the main features of the new device generation. Third, the model is used for further optimisation of the device structure by individually designing the two DFB-corrugations.

Mathematical model: The slowly varying amplitudes $\Psi^\pm(z, t)$ of forward and backward travelling waves are obtained by numerically solving the travelling wave equations

$$v_{\text{group}}^{-1} \partial_t \Psi^\pm \pm \partial_z \Psi^\pm = -i\beta \Psi^\pm - i\kappa^\mp \Psi^\mp, \quad (1)$$

together with the rate equation for the carrier density in the gain section,

$$\frac{d}{dt} N = \frac{I_g}{eV_g} - (AN + BN^2 + CN^3) - g' (N - N_{tr}) \langle |\Psi^+|^2 + |\Psi^-|^2 \rangle_g. \quad (2)$$

Here $\langle \dots \rangle_g$ denotes averaging over the gain section. Other symbols have their usual meaning, the indexes g, p, r label the section they belong to. No coupling of carriers to the field appears for the phase and reflector sections because they are passive or at transparency, respectively. The relative propagation parameters β are treated as spatially constant within each section. In the reflector section (kept at transparency), only the optical losses contribute, $\beta_r = -i\alpha_r/2$. A static detuning δ as well as the carrier induced detuning and gain terms appear additionally in the gain section, $\beta_g = \delta - i\alpha_g/2 + (\alpha_H + i)g' [N - N_{tr}]/2$. For the phase tuning section we use $\beta_p = -\varphi/2L_p - i\alpha_p/2$ with the variable phase angle φ . The parameter values of [4] are used except $\alpha_p = 20 \text{ cm}^{-1}$, $A = 3 \times 10^8 \text{ s}^{-1}$, $B = 10^{-10} \text{ cm}^3/\text{s}$, $C = 10^{-28} \text{ cm}^6/\text{s}$.

Evaluation of the model: We have checked the validity of the new model by comparing with measured features of the present device generation as well as with Marcenac's model

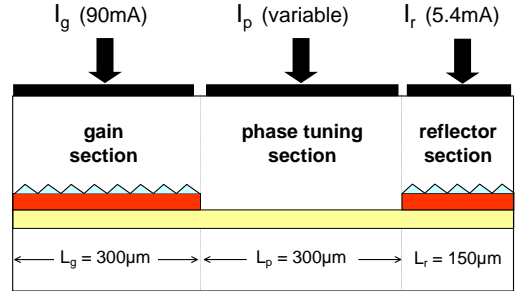


Figure 1: Scheme of a typical device.

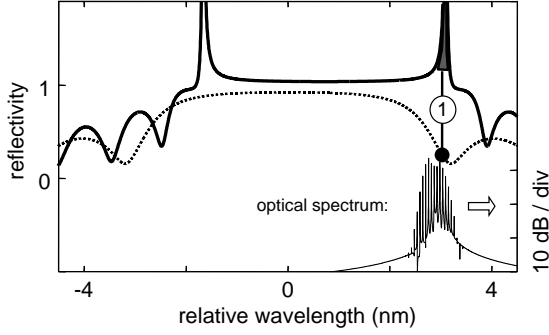


Figure 2: Reflectivity spectra of the gain section (solid) and the reflector section (dashed) for one moment of a SP. Thin: calculated optical spectrum.

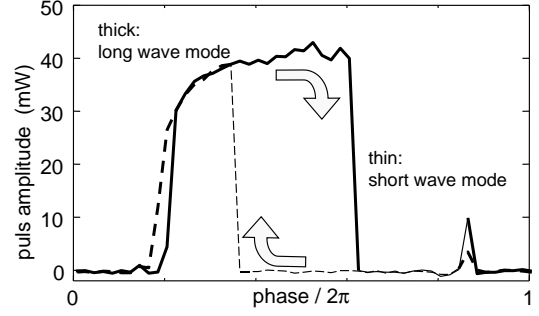


Figure 3: Amplitude of the SP calculated for increasing (solid) and decreasing (dashed) phase angle. Thick: long wave mode lasing as ① in Fig. 2, thin: short wave mode lasing.

[5]. SP have been obtained for the same conditions as in the experiment. First, a typical *spectral correlation* is required: the lasing resonance of the gain section has to coincide with the negative reflectivity slope of the reflector section (Fig. 2). The combination of electronic blue and thermal redshift with increasing current allows to adjust to such a position [3]. Second, the SP are switched on and off by *phase current tuning* (Fig. 3).

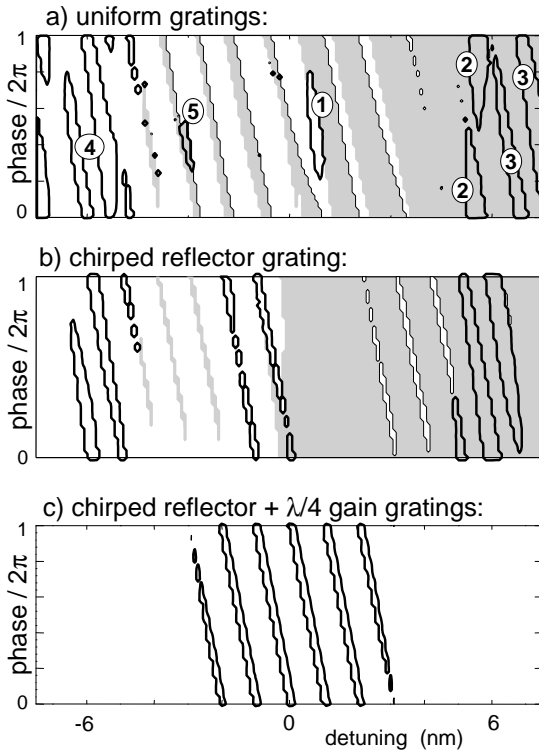


Figure 4: Thick: areas of SP in the $\delta - \varphi$ plane for differently styled DFB gratings. Grey background: short wave mode lasing. White background: long wave mode lasing.

obtained are drawn in Fig. 4a as islands with thick black borders. Island ① in the center belongs to the spectral correlation of Fig. 2 and can be addressed by the thermal λ -shift in the present generation of devices discussed above. For larger detunings, several new SP islands appear (note that islands touching the border $\varphi = 2\pi$ continue at $\varphi = 0$ and vice versa, due to the phase periodicity). The reflectivity spectra drawn in Fig. 5 for the islands ② to ⑤ show that

A distinct hysteresis appears at one side of the SP region. In this range, either mode of the gain section may carry the lasing power. The long wave mode shows SP, whereas the short wave mode is stationary. Hysteresis and mode jumps have been observed in the experiments, too, but they appeared less pronounced. We attribute this small difference to neglecting the gain dispersion in the model. The calculated SP frequencies are in the 10 GHz range and depend on the gain current and the phase angle as in the experiments. Summarizing so far, our new model describes well the main features of the self pulsating devices with the reflector section at gain transparency.

Device optimisation by grating design:

First, we investigated devices with *detuned gratings*, i.e., with different corrugation periods for the gain and reflector sections. The according detuning parameter δ of the model has been varied over a 15 nm wide range with steps of 0.1 nm. For every δ , the phase angle φ was tuned upwards from 0 to 2π in 50 equidistant steps. The SP-regions obtained

they belong to other possible combinations of one of the two lasing modes with a negative slope of one of the different lobes of the reflector spectrum. Being larger and less sensitive to mode jumps, these islands are improved compared to island ①. Using first devices with detuned gratings, we could experimentally verify the existence of SP for large detuning.

In a next step, we introduced a tapered grating $\kappa = \kappa_0 \cos^2(\pi z/L_r)$ in the reflector section ($z = 0$: center of the section). This suppresses considerably the side lobes of its reflectivity. As a consequence, all SP islands connected with side lobes disappear (Fig. 4b). The former central island ① reappears a bit short wave shifted in a wider tuning range due to the smaller and smoother stop band of the tapered reflector. The island around 6 nm is the most prominent one. It is a coalescence of the former islands ② and ③, resulting in a much wider continuous tuning range. The sensitivity to mode jumps is not further reduced as indicated by the continuation of the SP islands into mode jump islands. Surprisingly, an additional SP island is situated around -6 nm. Here, the right mode lases on the positive slope of the reflectors stop band. This exception from our usual picture of dispersive self-Q switching [3] was also observed with the simulation tool OPALS [6] and is still under investigation.

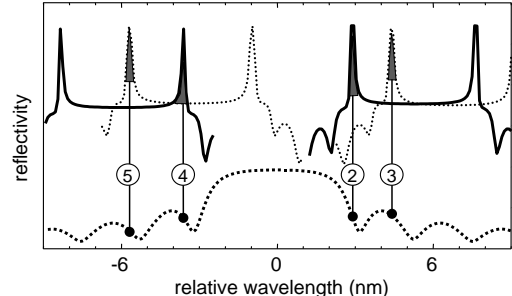


Figure 5: Spectral correlations for some prominent SP islands of Fig. 4a.

Finally, we additionally introduced a quarterwave shift into the gain section. As expected, there is no mode jump in the whole area of calculation. Furthermore, a single distinct SP island appears (Fig. 4c) with SP frequencies also in the 10 GHz range. This island covers an about 6 nm wide region in the center of the tuning range, which seems very useful for the device functionality. The detailed nature of these SP as well as their dependence on parameters have to be further investigated.

Conclusion: High-speed self-pulsations can be generated with rather different grating designs. The following possible improvements of the present generation of devices were found: Detuned gratings lead to broader SP regions with less tendency to mode switching. A tapered reflector grating reduces the variety of SP regions to few well pronounced areas. One single extended SP area without mode hopping can be obtained by additionally introducing a quarterwave shift into the gain section.

Acknowledgement: We thank D. D. Marcenac to let us have his computer code [5].

References

- [1] M. Möhrle, U. Feiste, J. Hörer, R. Molt, and B. Sartorius, "Gigahertz self-pulsations in 1.5 μm wavelength multisection DFB lasers," *IEEE Photon. Technol. Lett.* **4**, pp. 976-979, 1992.
- [2] B. Sartorius, C. Bornholdt, O. Brox, H. J. Ehrke, D. Hoffmann, R. Ludwig, and M. Möhrle, "All-optical clock recovery module based on a self-pulsating DFB laser," *Electron. Letters* **34**, pp. 1664-65, 1998.
- [3] B. Sartorius, M. Möhrle, S. Reichenbacher, H. Preier, U. Bandelow, and H.J. Wünsche, "Dispersive self Q-switching in self-pulsating DFB lasers," *IEEE Journ. of Quantum Electronics* **33**, pp. 211-18, 1997.
- [4] U. Bandelow, H.J. Wünsche, B. Sartorius and M. Möhrle "Dispersive Self-Q-Switching in DFB Lasers – Theory Versus Experiment", *IEEE J. Selected Topics in Quantum Electronics* **3**, pp. 270-278, 1997.
- [5] D. D. Marcenac, "Fundamentals of laser modelling", *Dissertation, St. Catharine's College, University of Cambridge*, 1993; D. D. Marcenac and J. E. Carroll, "Distinction between multimoded and singlemoded self-pulsations in DFB lasers," *Electron. Lett.* **30**, pp. 1137-1138, 1994.
- [6] H.-P. Nolting, "Modeling of all optical functional devices for signal processing: 3R-regenerators", invited to IPR 99.